Fission yeast Cyk3p is a transglutaminase-like protein that participates in cytokinesis and cell morphogenesis

Luther W. Pollard[a], Masayuki Onishi[b], John R. Pringle[b], and Matthew Lord[a]
[a]Department of Molecular Physiology & Biophysics, University of Vermont, Burlington, VT 05405; [b]Department of Genetics, Stanford University School of Medicine, Stanford, CA 94305

ABSTRACT **Cell morphogenesis is a complex process that relies on a diverse array of proteins and pathways. We have identified a transglutaminase-like protein (Cyk3p) that functions in fission yeast morphogenesis. The phenotype of a *cyk3* knockout strain indicates a primary role for Cyk3p in cytokinesis. Correspondingly, Cyk3p localizes both to the actomyosin contractile ring and the division septum, promoting ring constriction, septation, and subsequent cell separation following ring disassembly. In addition, Cyk3p localizes to polarized growth sites and plays a role in cell shape determination, and it also appears to contribute to cell integrity during stationary phase, given its accumulation as dynamic puncta at the cortex of such cells. Our results and the conservation of Cyk3p across fungi point to a role in cell wall synthesis and remodeling. Cyk3p possesses a transglutaminase domain that is essential for function, even though it lacks the catalytic active site. In a wider sense, our work illustrates the physiological importance of inactive members of the transglutaminase family, which are found throughout eukaryotes. We suggest that the proposed evolution of animal transglutaminase cross-linking activity from ancestral bacterial thiol proteases was accompanied by the emergence of a subclass whose function does not depend on enzymatic activity.**

Monitoring Editor
Rong Li
Stowers Institute

Received: Jul 29, 2011
Revised: Apr 26, 2012
Accepted: May 3, 2012

INTRODUCTION

Transglutaminases (TGases) are a family of enzymes that catalyze intramolecular or intermolecular protein cross-linking through isopeptide bond formation between lysine (or polyamines) and glutamine residues. The activity of the enzymes plays an important role in various intracellular and extracellular processes. For example, keratinocyte TGase functions in the terminal differentiation of keratinocytes and formation of the cornified cell envelope (Rice and Green, 1978; Thacher and Rice, 1985); tissue TGase (TG2) is found in many cell types and is involved in inflammation, apoptosis, cell adhesion, and cancer and other human diseases (Fesus and Szondy, 2005; Mangala and Mehta, 2005; Mehta *et al.*, 2010; Facchiano *et al.*, 2006; Zemskov *et al.*, 2006). Factor XIII probably represents the best-studied TGase; it participates in blood clotting, tissue repair, and wound healing (Pisano *et al.*, 1968; Schwartz *et al.*, 1973; Mosher and Schad, 1979; Sakata and Aoki, 1980; Knox *et al.*, 1986). A hallmark of these enzymes is a catalytic triad made up of conserved cysteine, histidine, and aspartate residues, each of which is essential for activity and defines the catalytic core (Figure 1A; Hettasch and Greenberg, 1994; Micanovic *et al.*, 1994; Pedersen *et al.*, 1994; Yee *et al.*, 1994).

The increasing abundance of protein sequence information has revealed a new inactive class of TGases that possesses a conserved catalytic domain lacking the catalytic triad (Makarova *et al.*, 1999). For example, a red blood cell protein (band 4.2) possesses a TGase domain that lacks the catalytic cysteine and histidine residues (Figure 1A) and consequently lacks enzyme activity (Korsgren *et al.*, 1990; Cohen *et al.*, 1993). Naturally occurring mutations in the human

This article was published online ahead of print in MBoC in Press (http://www.molbiolcell.org/cgi/doi/10.1091/mbc.E11-07-0656) on May 9, 2012.

Address correspondence to: Matthew Lord (matthew.lord@uvm.edu).

Abbreviations used: DIC, differential interference contrast; EM, electron microscopy; EMM, Edinburgh minimal medium; FRAP, fluorescence recovery after photobleaching; GFP, green fluorescent protein; MEN, mitotic exit network; NA, numerical aperture; ORF, open reading frame; ROI, region of interest; SIN, septation initiation network; SPB, spindle-pole body; TGase, transglutaminase; YE5S, yeast extract plus supplements.

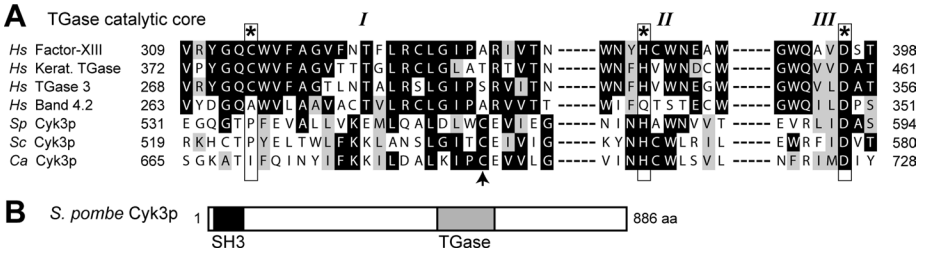

FIGURE 1: Conserved protein domains of Cyk3p. (A) A sequence alignment comparing identities (black) and similarities (gray) among amino acids from four human transglutaminases and three Cyk3p homologues (*Sp*: fission yeast *S. pombe*; *Sc*, *Ca*: budding yeasts *S. cerevisiae* and *C. albicans*). The alignment centers on the active-site cysteine (motif I), histidine (II), and aspartate (III) residues (asterisks) forming the conserved catalytic triad in the transglutaminase core. The variable regions (dashed lines) between motifs I and II span 32 residues for the human transglutaminases (except TGase 3: 31 residues) and 14 residues for the Cyk3p proteins (except *Sc*: 12 residues); the variable regions between motifs II and III span 11 residues for human transglutaminases and 3 residues for the Cyk3p proteins. The arrowhead marks a cysteine residue (Cys-554 in *S. pombe*) conserved among the Cyk3p proteins. (B) Position of the SH3 (amino acids 10-65) and transglutaminase-like (amino acids 485-595) domains in the 886-residue fission yeast Cyk3p sequence. The domains were identified using the Blastp program.

band 4.2 gene cause congenital spherocytic anemia characterized by sphere-shaped (rather than biconcave disk–shaped) cells that are more prone to hemolysis (Yawata, 1994; Bruce *et al.*, 2002; Dahl *et al.*, 2004). This phenotype highlights the physiological relevance of proteins with inactive TGase domains, and may reflect a structural role at the cell membrane in the case of band 4.2 (Satchwell *et al.*, 2009). However, nothing is known regarding the cellular role (if any) of the inactive TGase domains themselves. In this study, we examined the role of an inactive TGase (Cyk3p) from the fission yeast *Schizosaccharomyces pombe*.

Cyk3p was originally identified in the budding yeast *Saccharomyces cerevisiae* (Korinek *et al.*, 2000), and (based on available sequence data) represents a highly conserved fungal protein. Cyk3p participates in cytokinesis in *S. cerevisiae* (Korinek *et al.*, 2000), and was recently found to be essential for cytokinesis and growth in the pathogenic budding yeast *Candida albicans* (Reijnst *et al.*, 2010). Several studies in *S. cerevisiae* recently shed light on the molecular mechanisms governing Cyk3p function. Localization of Cyk3p at the division site depends on its N-terminal SH3 domain (Jendretzki *et al.*, 2009), which mediates an interaction with a proline-rich region at the C-terminus of the C2 domain protein (Inn1p), a critical cytokinetic factor (Sanchez-Diaz *et al.*, 2008; Jendretzki *et al.*, 2009; Nishihama *et al.*, 2009). Cell cycle–specific phosphorylation may regulate such complexes, because the division site localization of Cyk3p and Inn1p relies on the mitotic exit network (MEN; Meitinger *et al.*, 2010), a conserved signaling pathway essential for the coordination of mitotic progression and cytokinesis (McCollum and Gould, 2001). Relatively little is known about fission yeast Cyk3p, although preliminary studies have pointed to a role in cytokinesis. Similar to several other fission yeast cytokinetic mutants, a *cyk3*Δ mutant was found to be sensitive to loss of the cytokinetic checkpoint mediated by the Cdc14 family phosphatase (Mishra *et al.*, 2004). In addition, fission yeast Cyk3p was recently found to coprecipitate from cell extracts with F-BAR protein Cdc15p (Roberts-Galbraith *et al.*, 2010), an essential component of the contractile ring (Fankhauser *et al.*, 1995).

In this study, we define roles for Cyk3p in fission yeast cytokinesis and morphogenesis and identify an inactive C-terminal TGase motif as the critical functional element. Overall, our study provides new insights into the mechanisms of Cyk3p function, cytokinesis, and cell morphogenesis in fungi, and more broadly identifies an important cellular role for the inactive subclass of the TGase family.

RESULTS

Fission yeast Cyk3p functions in cytokinesis and morphogenesis

Like other known fungal members of this protein family (Korinek *et al.*, 2000; Reijnst *et al.*, 2010), fission yeast Cyk3p possesses an N-terminal SH3 domain (Figure 1B). In addition, we identified a TGase-like domain in the C-terminal half of the protein (Figure 1B), a domain preserved in Cyk3p sequences from other fungi. This 111–amino acid domain showed homology to TGase domains in *S. cerevisiae* Cyk3p (30% identical/51% similar) and animal TGases (e.g., 17%/41% vs. human factor XIII). The catalytic core of the TGase domain can be separated into three motifs centered on the conserved cysteine, histidine, and aspartic acid active-site residues that form the catalytic triad. Interestingly, the catalytic triads of the fungal Cyk3p proteins are all incomplete, containing the conserved histidine and aspartic acid residues in motifs II and III but lacking the active site cysteine in motif I (Figure 1A).

Deletion of *cyk3* had no obvious effect on morphology or growth at 25–32°C. However, *cyk3*Δ cells exhibited temperature-sensitive defects in cell separation at 36°C, as reflected by the appearance of elongated cells with multiple septa and multiple nuclei (Figure 2A). In addition, *cyk3*Δ cells showed a greater tendency to adopt a rounded/swollen morphology, as opposed to the typical cigar shape of fission yeast (Figure 2A). Consistent with a significant role for Cyk3p in cytokinesis, the *cyk3*Δ mutation showed synthetic defects when combined with mutations in genes encoding known contractile ring components, such as Myo2p (myosin II), Cdc4p (essential light chain), Cdc12p (formin), and Cdc15p (F-BAR protein) (Figure 2, B and C, and Supplemental Figure S1). Although the contractile rings typically assembled in such double mutants, they showed obvious defects in cytokinesis (Figure 2D), suggesting a role for Cyk3p in ring constriction.

Surprisingly, unlike *myo2-E1* and many other cytokinetic mutations (Bezanilla *et al.*, 1997; Motegi *et al.*, 1997), *cyk3*Δ did not exhibit synergistic cytokinetic defects when combined with a *myp2* null (Figures 2E and S1). Myp2p is a nonessential myosin II required for normal cytokinesis (Bezanilla *et al.*, 1997; Motegi *et al.*, 1997), and the lack of an additive phenotype suggests that Cyk3p and Myp2p may share a specific function in cytokinesis. Myp2p is known to associate with chitin synthase (Chs2p), an inactive form of the enzyme that localizes to the contractile ring and contributes to septum formation in fission yeast (Martin-Garcia *et al.*, 2003; Martin-Garcia and Valdivieso, 2006). We therefore also examined a *cyk3*Δ *chs2*Δ double mutant. Interestingly, loss of Chs2p completely suppressed the cytokinetic defects associated with loss of Cyk3p (Figures 2F and S1), suggesting a functional relationship between these two proteins at the septum.

Cyk3p localizes to the contractile ring, division septum, and sites of polarized growth

We used gene replacement to generate single and triple chromosomal green fluorescent protein (GFP) fusions to examine the subcellular localization of endogenous Cyk3p. The fusion proteins were functional based on their ability to fully support Cyk3p function in a

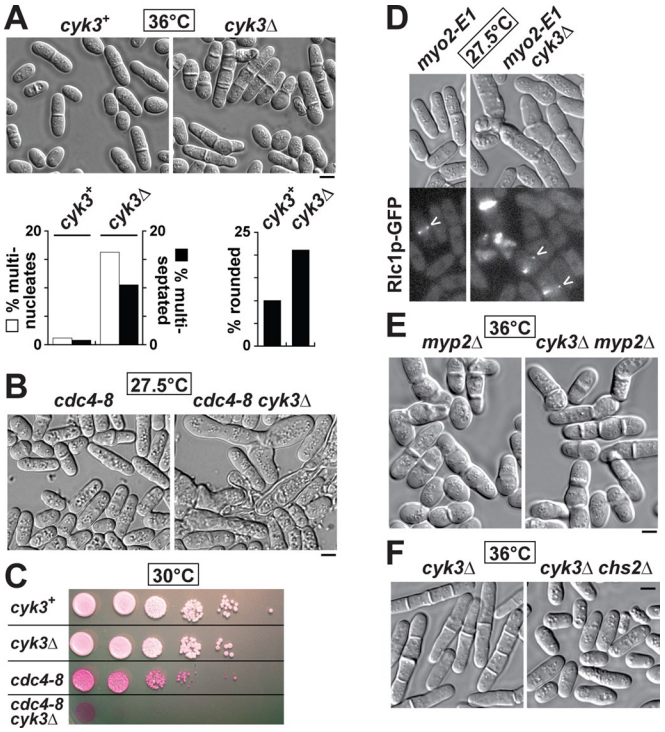

FIGURE 2: Cyk3p functions in cytokinesis and polarized growth. (A) Representative DIC images of wild-type (MLP 11) and *cyk3*Δ (MLP 3) cells following growth at 36°C in YE5S medium. Plots below provide quantification of morphological defects observed under these conditions. Left, percentages of multinucleate cells (following treatment with 4′,6-diamidino-2-phenylindole stain: 3+ nuclei/cell, □; n = 750) and of cells possessing >1 division septa, ■ (which account for the majority of multinucleate cells). Right, percentages of cells with a rounded/swollen shape (n = 750). (B) Representative *cdc4-8* (TP 6) and *cdc4-8 cyk3*Δ (MLP 178) cells following growth at 27.5°C on YE5S medium. (C) Growth of wild-type, *cyk3*Δ, *cdc4-8*, and *cdc4-8 cyk3*Δ strains at 30°C. Five-microliter cell suspensions of identical optical density were spotted along with five 10-fold serial dilutions onto a YE5S plates. The plate contained 5 μg/ml phloxin B, a pink dye that accumulates inside dead cells (note the pink color of the *cdc4-8* and *cdc4-8 cyk3*Δ colonies). (D) Representative *myo2-E1* (TP 73) and *myo2-E1 cyk3*Δ (MLP 17) cells following growth at 27.5°C on YE5S medium. Top panels, DIC images; bottom panels, Rlc1p-GFP localization at rings (as denoted by arrowheads). (E) Representative *myp2*Δ (MLP 34) and *myp2*Δ *cyk3*Δ (MLP 35) cells following growth at 36°C on YE5S medium. (F) Representative *cyk3*Δ and *cyk3*Δ *chs2*Δ (LP 112) cells following growth at 36°C on YE5S medium. Counts of the percentages of multinucleate cells for the strains shown in (B), (D), (E), and (F) are provided in Figure S1.

cdc4-8 background. During vegetative growth, Cyk3p localized to three distinct sites: contractile rings, division septa, and cell tips (Figure 3A). The Cyk3p signal was most prominent at contractile rings. Time-lapse analysis revealed that Cyk3p joins the ring at the final stages of its assembly, is present at both rings and across growing septa during ring constriction, and remains as a band spanning the septum following ring disassembly (Figure 3B). This pattern was particularly clear when Cyk3p was colocalized with the myosin II regulatory light chain Rlc1p, which assembles earlier and disappears following ring contraction (Figure 3C and Supplemental Movie S1).

On contractile ring disassembly, Cyk3p localization at the septum was relatively faint, but it became brighter a short time later, forming a tight spot at the center of the septum just before cell separation and remaining at the new cell poles following separation (Figure 3, A and D). This unipolar tip localization became bipolar as Cyk3p accumulated at the old cell poles later in the cell cycle (Figure 3D). Although the bipolar tip localization was relatively faint when the tagged Cyk3p was expressed at endogenous levels, it became more conspicuous when Cyk3p-GFP was expressed from a multicopy plasmid (Figure 3E).

In summary, Cyk3p localizes in a manner consistent with roles in cell morphogenesis during both division and polarized cell growth.

Cyk3p is a component of the contractile ring and promotes ring dynamics

Given its prominent localization at the actomyosin ring, we tested whether Cyk3p was truly a component of this structure. Fluorescence recovery after photobleaching (FRAP) studies have shown that ring components exchange rapidly and that myosin II Myo2p exchanges with different kinetics in nonconstricting and constricting rings (Sladewski *et al.*, 2009; Stark *et al.*, 2010). Examination of Cyk3p-GFP exchange revealed almost identical kinetics to those of Myo2p in both nonconstricting ($t_{½}$ = 27 s vs. ~37 s for Myo2p), and constricting ($t_{½}$ = 12 s vs. ~13 s for Myo2p) rings (Figure 4, A and B; Sladewski *et al.*, 2009). Depolymerization of the actin cytoskeleton with latrunculin A blocked the formation of both myosin II and Cyk3p rings and led to a buildup of both proteins as ring precursors at the incipient medial division sites (Figure 4C). Taken together, these results suggest that Cyk3p is indeed a component of the actomyosin ring.

To test for a possible role of Cyk3p in contractile ring dynamics, we first monitored contractile ring behavior, using Rlc1p-GFP as a marker, in relation to mitotic progression, as judged by the spindle-pole body (SPB) protein Sad1p-GFP (Figure 5A, left box). Using the beginning of SPB separation as a reference point, we found that ring assembly time and constriction rate were affected little or not at all in a *cyk3Δ* mutant grown at 25°C, whereas the preconstriction "dwell" time was significantly lengthened (Figure 5, A and B, and Table 1). Interestingly, the delay was paralleled by a delay in the completion of spindle elongation: although ring constriction began ~8–9 min following spindle breakdown in both wild-type and *cyk3*Δ cells, spindle breakdown (like ring constriction) was delayed ~6 min in the mutant relative to wild-type (Figure 5B). The reason for this delay is not clear, but it appeared to be due mostly to a slower spindle elongation during the phase of contractile ring assembly (Figure 5B).

The ability of *cyk3Δ* cells to grow at 36°C allowed a further informative analysis in which cells grown at 36°C were subsequently imaged at 23°C. In this case, the assembly, dwell, and constriction phases were all significantly affected, with the largest effect on the dwell time (Figure 5C and Table 1), probably because the absence of Cyk3p during growth at 36°C produced changes in the levels of Cyk3p-interacting proteins that could affect ring dynamics even after a return to lower growth temperature. In summary, although Cyk3p appears to be involved in all phases of contractile ring function, its most important role seems to be in promoting ring constriction.

Cyk3p participates in cell separation following disassembly of the contractile ring

The localization of Cyk3p to the septal region (Figure 3) and multiseptate phenotype of *cyk3Δ* mutants (Figure 2A) suggested Cyk3p might play a role in the maturation of the septum, its splitting at cell division, or both. Consistent with such a role(s), *cyk3Δ* cells showed increased percentages of septated cells (Figure 6A) and of cells that apparently failed to separate (Figure 6B), as well as an increase

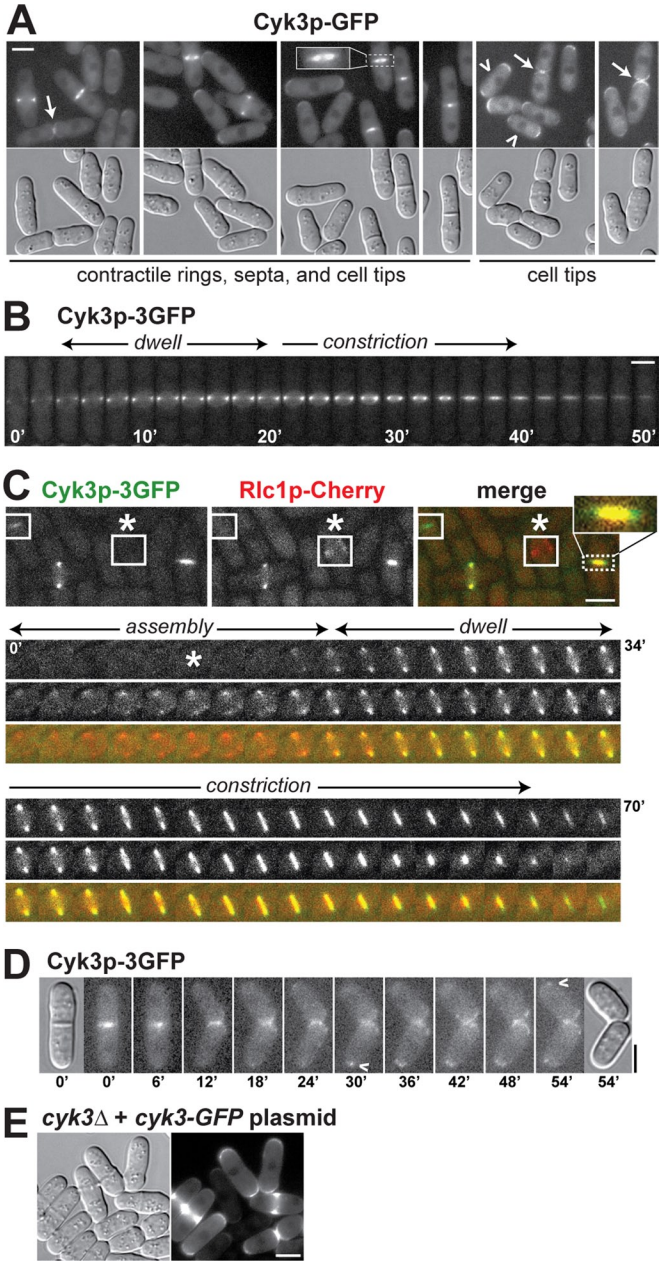

FIGURE 3: Cyk3p localization dynamics during cell division and growth. (A) Localization of Cyk3p-GFP to contractile rings, septa, and cell tips (in strain MLP 15). Box, magnification of the division site of a cell undergoing ring constriction and septation; arrows, Cyk3p appearing at newly formed cell tips during cell separation; arrowheads, Cyk3p visible at both cell poles in separated cells. (B) Time-lapse observations of Cyk3p-3GFP (LP 37) at the division site from completion of ring assembly to shortly after ring disassembly. (C to D) Colocalization of Cyk3p and the myosin II RLC. (C) Representative cells (MLY 757) illustrating the distinct localization profiles of Cyk3p-3GFP (left and green in merge) and Rlc1p-Cherry (center and red in the merge). Left box, a cell showing the continuing presence of Cyk3p at the division site following disappearance of the contractile ring; center box, absence of Cyk3p during ring assembly; right box in merge, overlapping Cyk3p and Rlc1p signals in the contractile ring (yellow) and the relatively faint Cyk3p signal in the septum surrounding the ring (green). (A time-lapse movie of this field of cells is provided in Movie S1.) Bottom panels, time-lapse observations showing the localization patterns of Cyk3p and Rlc1p. The 10-min image (asterisk) corresponds to the assembling-ring stage, as marked with an asterisk in (C). (D) Time-lapse observations of Cyk3p-3GFP localization from 12 min after completion of ring constriction and septation, which is also 12 min before cell separation. (E) Cyk3p-GFP localization following expression from a multi-copy plasmid with *cyk3-GFP* under control of the weak-strength *81nmt1*-inducible promoter. *cyk3*Δ cells were transformed and grown in EMM lacking uracil at 30°C. Scale bars (A–E): 4 μm.

in the average time from septum completion to cell separation (Figure 6, C and D), during growth at 36°C. These effects were not seen at 25°C (Figure 6D), and even at 36°C, septum completion appeared to coincide with the completion of contractile ring constriction, as in wild-type cells (Figure 6C). Thus, in addition to a role in actomyosin ring constriction, Cyk3p also contributes to cell separation.

Cyk3p concentrates in dynamic cortical puncta during stationary phase

When cells expressing Cyk3-GFP grew to stationary phase, they displayed a pattern of localization that appeared to be distinct from the division site and cell tip localization seen during vegetative growth. In particular, Cyk3p was found randomly throughout the cortex as discrete, dynamic puncta (Figure S2 and Movies S2 and S3). Although these puncta were similar in size and distribution to endocytic actin patches, Cyk3p did not colocalize with the actin-patch component Fim1p (fimbrin) during stationary phase (Figure S2), and the Cyk3p puncta had a considerably longer average lifetime (~4 min) than did Fim1p or actin patches (~20 s; Figure S2; Sirotkin *et al.*, 2010). In addition, unlike typical endocytic patches, the Cyk3p puncta did not depend on actin (Figure S2) and often showed considerable lateral motility (Movies 2 and 3). These observations suggest that Cyk3p may play a more general role in cell-surface organization in addition to its roles at specific sites during the vegetative cell cycle.

Overexpression of Cyk3p leads to defects in cytokinesis and cell shape

To explore further the roles of Cyk3p in vegetative cells, we overexpressed it in otherwise wild-type cells. On overexpression, cells displayed gross morphological defects characterized by multinucleate cells with abnormal septa and rounded/swollen shapes that had lost the typical cigar shape of fission yeast (Figures 7 and S3). A combination of both phenotypes was evident in some cells (Figure 7), but time-lapse observations revealed that the phenotypes were often independent of one another (Figure S3), so that cell swelling was not simply a secondary effect of cytokinetic failure. These phenotypes paralleled those of *cyk3*Δ cells (Figure 2A), presumably reflecting roles for Cyk3p in both cytokinesis and cell shape determination.

Cyk3p function depends on its transglutaminase domain but not its SH3 domain

To gain insight into Cyk3p function, we created plasmids expressing proteins that lacked the SH3 domain or contained mutations in the transglutaminase domain (see *Materials and Methods*). Surprisingly, Cyk3p-SH3*Δ* appeared to retain full function during cytokinesis (Figure 8, A and B) and to support normal polarized growth (Figure 8A). Moreover, like wild-type, this truncated form localized normally (Figure 8C), produced cytokinetic defects and morphological abnormalities when overexpressed (Figure 8D), and was expressed at normal levels (Figure 8E). In contrast, mutation of the conserved aspartate residue of the catalytic triad (in the TGase core) led to a seemingly complete loss of Cyk3p function (Figure 8, A, B, and D), even though the protein localized normally (Figure 8C) and was

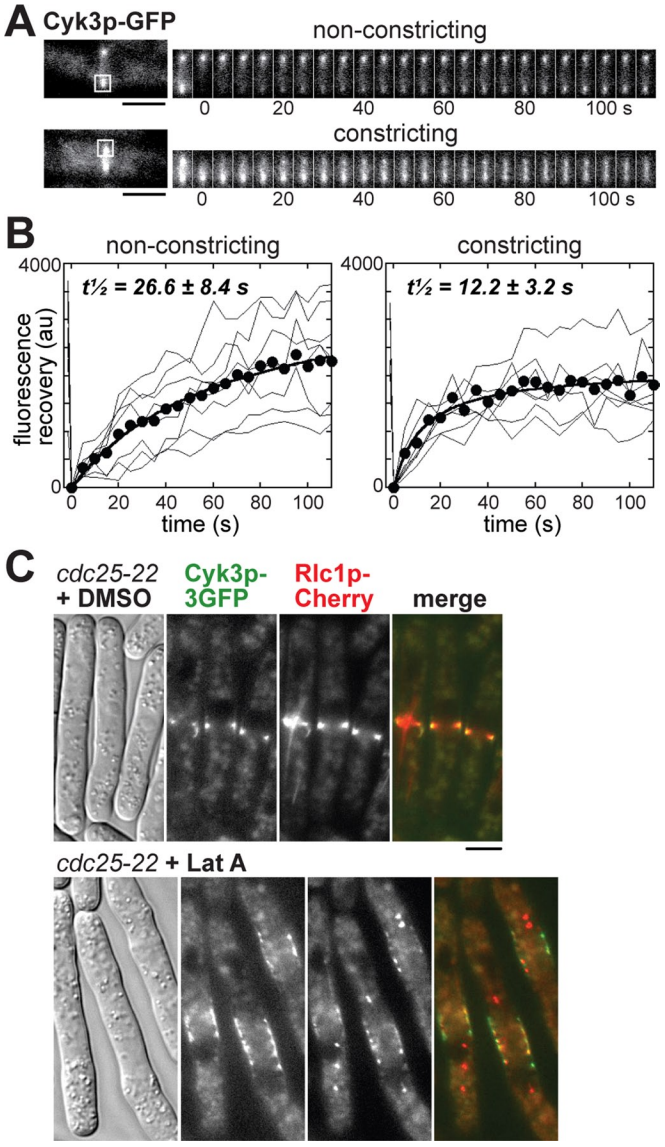

FIGURE 4: Cyk3p is a contractile ring component. (A and B) Measurement of Cyk3p exchange rates in contractile rings using FRAP. *cyk3-GFP* (MLP 15) cells were grown in YE5S medium at 25°C and examined at room temperature, as described in *Materials and Methods*. (A) Representative images comparing the recovery of Cyk3p-GFP fluorescence in nonconstricting (top) and constricting (bottom) rings. Left, cells before bleaching; the ROIs (white boxes) were then bleached at time zero. Right, recovery of signal over 110 s after bleaching. (B) Quantitation of FRAP in experiments like those in (A). Fluorescence intensities measured prebleach (–1.5 s) and postbleach (every 5 s for 0–110 s) are plotted. Individual ROI traces (thin lines) are shown (n = 7–8) along with the averages (filled circles, thick line). (C) Cyk3p ring assembly relies on actin filaments. Cells (LP 116) were arrested at the G2 phase of the cell cycle by invoking the temperature-sensitivity of the *cdc25-22* mutation via 4 h of growth at 36°C. Cells were released from the arrest by growth at 25°C for 30 min in the presence of dimethyl sulfoxide (control) or 10 μM latrunculin A to prevent actin polymerization and contractile ring formation. In the presence of latrunculin, Cyk3p and myosin II (Rlc1p-Cherry) localize at the division site in (actin-independent) broad bands. Scale bars (A, C): 4 μm.

expressed at normal levels (Figure 8E). We further tested the importance of the TGase domain using another mutation (His-577-Ala) in the catalytic triad (Figure 1). This mutant protein was expressed effectively, localized normally, and rescued the growth of a *cdc4-8 cyk3Δ* mutant (Figures 8E and S4). However, closer inspection revealed that Cyk3p-His-577-Ala retained only partial function: it was unable to fully relieve the morphological and cytokinetic defects associated with loss of Cyk3p, and it produced relatively mild morphological defects when overexpressed (Figure S4). In summary, the TGase domain, but not the SH3 domain, is critical for Cyk3p function in fission yeast.

Cyk3p links the contractile ring and division septum during cytokinesis

Contractile ring constriction and septum formation are coupled in yeast. The unique localization of Cyk3p in both rings and septa prompted us to further examine its roles in these structures. Because *S. cerevisiae* Cyk3p division site localization depends on the MEN pathway (Meitinger *et al.*, 2010), we tested whether the homologous pathway (the septation initiation network, or SIN) governed Cyk3p localization in fission yeast. The SIN is essential for initiating septum formation and ring constriction (McCollum and Gould, 2001). Use of a temperature-sensitive *sid2-250* mutant demonstrated that localization of Cyk3p to rings was not dependent on the SIN (Figure S5). Thus, as with other contractile ring proteins, the formation of Cyk3p rings is actin-dependent (Figure 4C) but does not rely on septum formation. This indicates that Cyk3p is a core component of the ring that must interface with the leading edge of the trailing septum during cytokinesis, presumably leading to its incorporation across the septum (Figure 3C).

We turned to electron microscopy (EM) to directly assess Cyk3p's role in ring constriction and septation, and, in particular, how the contractile ring defects of *cyk3* mutants affected growth of the septum. Although septation was generally normal in the absence of Cyk3p (Figure 9A, compare a–d with e–g; Figure 9C), a few *cyk3Δ* cells (3 of 114 cells examined) contained an apparently complete septum with a gap in the electron-translucent central layer (Figures 9Ah and 9C) that was never observed in wild-type cells. Actomyosin ring mutants also displayed defects in septum structures (Figure 9B, a, b, f, and g), which became much more severe in double mutants lacking *cyk3Δ* (Figure 9B, c–e and h–j). Although these double mutants were viable, their septa were typically abnormally thickened and often appeared misdirected across the division plane (Figure 9, B and C). Consistent with the genetic data indicating that Cyk3p functions in the same pathway as Myp2p (Figures 1E and S1), the EM analysis revealed little or no exacerbation of the *myp2Δ* septation defect by loss of Cyk3p (Figures 9C and S6). Taken together with the localization of Cyk3p, these direct observations of the septa imply a role for Cyk3p in coupling ring constriction and septum growth during cytokinesis.

DISCUSSION

Our work highlights the role of a TGase-related protein in cell morphogenesis. Fission yeast Cyk3p participates in actomyosin ring constriction, septation, and cell separation during cytokinesis, and also plays a relatively minor role in cell shape and integrity during vegetative growth and stationary phase. Inactive TGases such as Cyk3p are found throughout eukaryotes and our results demonstrate that the TGase domains of such proteins can have key roles in the cell.

Fission yeast Cyk3p functions in cytokinesis and cell wall remodeling

Cyk3p functions in cytokinesis, promoting ring constriction and subsequent cell separation. Correspondingly, Cyk3p appears in two

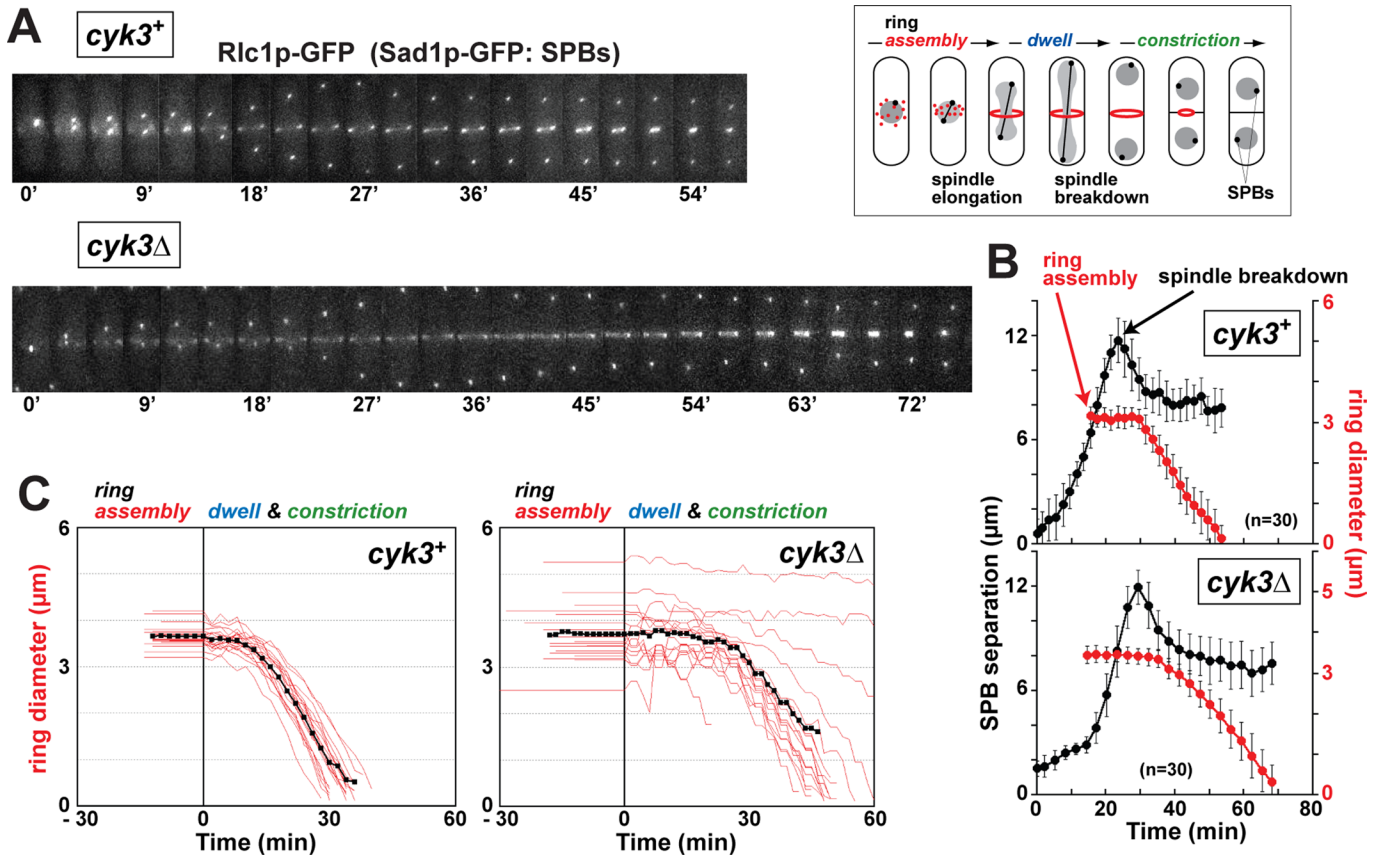

FIGURE 5: Cyk3p affects contractile ring dynamics. Ring dynamics and mitotic spindle behavior were assessed by tracking Rlc1p-GFP and Sad1p-GFP, respectively. (A) Time-lapse observations (maximum projections from six Z-sections captured every 3 min) on representative wild-type (MLY 572) and *cyk3Δ* (MLY 657) cells grown in YE5S medium at 25°C. The observations begin immediately before SPB separation. Right, schematic shows the normal timing of ring (red) assembly, dwell, and constriction phases relative to mitotic progression based on SPB dynamics. (B) Plots summarizing the results from wild-type and *cyk3Δ* cells examined as in (B). For each strain, mean ring diameters (red) and SPB separation distances (black) were aligned based on the times at which each ring initiated constriction, and time zero was defined as the mean time from initial SPB separation to initiation of ring constriction. The times at which ring assembly was completed and spindle breakdown began are indicated by arrows; error bars show standard deviations. Dwell phases (horizontal portion of curve) and constriction phases (diagonal portion of curve) are evident. Table 1 contains average values and statistics. (C) Traces showing the ring assembly, dwell, and constriction phases for 20 individual cells (red) and the corresponding means (black) from wild-type (MLP 198) and *cyk3Δ* (MLY 655) cells examined by time-lapse microscopy in YE5S medium at 23°C after growth in the same medium at 36°C. Time zero is defined as the completion of ring assembly for each cell and thus represents the transition from assembly to dwell phases. SPB analysis was not performed in cells pregrown at 36°C, because Sad1p-GFP fails to mark SPBs under these conditions.

distinct structures, the actomyosin ring and the division septum. Cyk3p is an integral component of the ring and is incorporated late in ring assembly. Around this time *cyk3Δ* cells exhibit a cell cycle delay reflected by a brief stall in anaphase B and a delay in the initiation of ring constriction. While the defects are subtle, *cyk3Δ* mutants (like other cytokinetic mutants) invoke lethality in the absence of the Cdc14 family phosphatase Clp1p/Flp1p (Mishra *et al.*, 2004). When ring integrity is compromised Clp1p activates a cytokinetic checkpoint, during which Clp1p activity is also mobilized to stabilize ring structures (Mishra *et al.*, 2004). Thus actomyosin rings lacking Cyk3p rely on compensatory maintenance to support cytokinesis and growth.

Although we do not yet understand the molecular mechanisms by which Cyk3p carries out its role at the ring, they probably involve three other factors: the F-BAR protein Cdc15p, the nonessential myosin II Myp2p, and the chitin synthase Chs2p. Cyk3p coprecipitates with Cdc15p from cell lysates and (along with other ring components) was found to accumulate at the division site upon premature self-assembly of a constitutively dephosphorylated form of Cdc15p (Roberts-Galbraith *et al.*, 2010). Our genetic analysis showed that *myp2Δ* was epistatic to *cyk3Δ*. Myp2p stabilizes rings as they constrict and ensures normal septation (Bezanilla *et al.*, 1997; Motegi *et al.*, 1997; Mulvihill and Hyams, 2003). Correspondingly, direct analysis of septation by EM in *myo2-E1 cyk3Δ* and *cdc4-8 cyk3Δ* double mutants indicated a role for Cyk3p in coordinating septum deposition with ring constriction. Chs2p is a transmembrane protein involved in septum formation and maintaining contractile ring integrity during the latter stages of constriction (Martin-Garcia *et al.*, 2003; Martin-Garcia and Valdivieso, 2006). The ability of the *chs2Δ* mutation to suppress cytokinetic defects associated with loss of Cyk3p suggests that Chs2p and Cyk3p work in a specific pathway with Myp2p. The actin-independent accumulation of Cyk3p at the division site probably relies on Cdc15p at ring precursors (nodes), given that Myp2p and Chs2p only localize to the division site once rings have formed (Bezanilla *et al.*, 2000; Martin-Garcia and Valdivieso, 2006).

Strain	Rlc1p-GFP ring property (± SD)[a]			
	Assembly (min)	Dwell (min)	Constriction (μm/min)	Lifetime[b] (min)
25°C				
cyk3$^+$	17.9 ± 3.1	15.0 ± 3.1	0.40 ± 0.05	42.5
*cyk3*Δ	18.6 ± 3.9	20.7 ± 5.7	0.35 ± 0.10	52.1
36°C				
cyk3$^+$	12.0 ± 1.7	12.6 ± 2.2	0.48 ± 0.05	35.5
*cyk3*Δ	18.5 ± 4.8	27.2 ± 14.0[c]	0.37 ± 0.10	56.9

[a]n = 50–73 rings/strain (25°C); n = 20 rings/strain (36°C). Altered ring properties (in wild-type vs. *cyk3*Δ cells) were confirmed by paired Student's *t* tests (in which a $p < 0.05$ indicates a significant difference between data sets). Ring assembly (36°C): p = 0.0023; dwell (25°C): $p < 0.0001$; dwell (36°C): p = 0.0002; constriction (36°C): p = 0.0003.

[b]Lifetimes are the sum of the average dwell and constriction times. Constriction time was estimated by dividing a representative contractile ring circumference (11 μm) by the average constriction rate.

[c]The relatively high SD for the *cyk3*Δ dwell time (36°C) reflects the protracted dwell phases observed in some cells. However, only rings that subsequently go on to complete constriction were included in the analysis.

TABLE 1: Influence of Cyk3p on contractile ring dynamics.

The actomyosin ring disassembles once ring constriction and septum formation are completed (Rajagopalan *et al.*, 2003). Completion of cytokinesis and cell separation occur a short time later upon septum maturation and subsequent digestion of the primary septum by the Eng1p and Agn1p endoglucanases (Martin-Cuadrado *et al.*, 2003; Dekker *et al.*, 2004). Cell separation was significantly

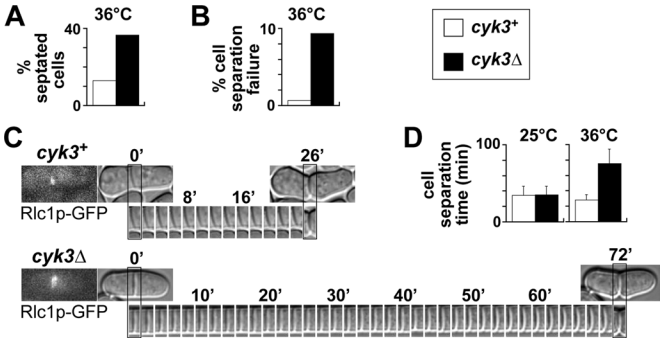

FIGURE 6: Cyk3p promotes cell separation. The role of Cyk3p was examined by comparing the efficiencies with which wild-type (MLP 198) and *cyk3*Δ (MLY 655) cells transitioned from septation to separation during growth on YE5S medium. (A and B) Histograms comparing the percentages of (A) cells with visible septa (n = 500) and (B) cell separation failure (n = 128–146) following growth at 36°C. Separation failure was defined as the failure of a septated cell to separate during the course of the 3-h time-lapse movie. Because *cyk3*Δ cells averaged 75.6 min from septum completion to cell separation during growth at 36°C (D), we only scored a cell as failing when a septum had been present >76 min by the end of the movie. (C) Single-cell images tracking medial division sites from septum completion (0′) to cell separation (defined as the loss of continuity between daughter cells as they split apart; see far right panels) for representative cells grown at 36°C. Completion of septation coincides with completion of contractile ring constriction (indicated by the fluorescence images of the disassembling Rlc1p-GFP ring, which is transiently observed at mid-cell as a smear following constriction). (D) Summary of average separation intervals (± SD) from experiments like those in (C), performed at 25 and 36°C (n = 11–15).

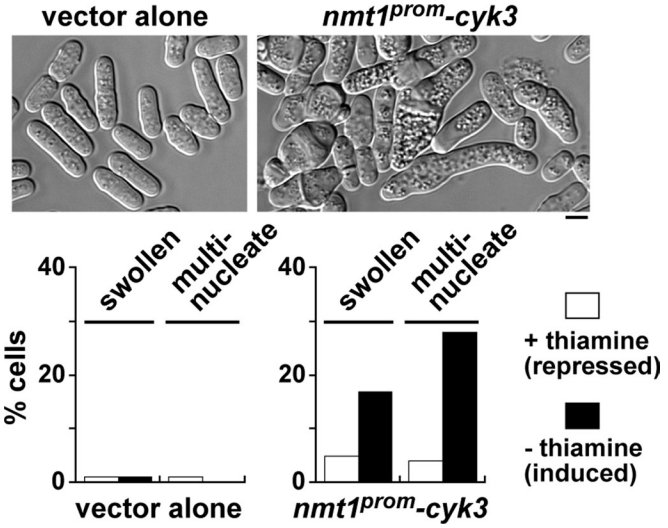

FIGURE 7: Cyk3p overexpression perturbs cell shape. Wild-type (MLP 11) cells were transformed with plasmid *nmt1*^{prom} (control) or *nmt1*^{prom}*-cyk3* (to overexpress Cyk3p from the full-strength *nmt1* promoter). Cells were grown initially on EMM-uracil plates containing 5 μg/ml thiamine, and were then resuspended in EMM- uracil liquid medium without thiamine and grown for 24 h to induce overexpression. Top, representative DIC images of control and Cyk3p-overexpressing cells. Bottom, such images were scored for the indicated abnormal cell morphologies (n = 500 for each count). Scale bars: 4 μm.

slower in *cyk3*Δ cells, suggesting an important role throughout this process for Cyk3p, consistent with its accumulation across the trailing septum during ring constriction and its polarization at the center of the septum immediately prior to cell separation. Outside of cytokinesis, Cyk3p localized at growing cell tips and redistributed throughout the cortex during stationary phase. These localizations and other results suggest that Cyk3p is mobilized for polarized growth during cell elongation and maintenance of cortical integrity upon cell cycle arrest and entry into the dormant phase. One consistent feature of Cyk3p localization is its appearance at the cortex during cell wall remodeling, both in growing cells and during stationary phase (when reinforcement and thickening of the wall occur to maintain cell integrity; Herman, 2002; Rincon *et al.*, 2006). Thus we hypothesize that Cyk3p is generally involved in facilitating cell wall synthesis and remodeling at relevant sites on the cortex.

Cyk3p: an inactive transglutaminase with physiological relevance

At a mechanistic level, how does Cyk3p contribute to morphogenesis? The SH3 domain of *S. cerevisiae* Cyk3p is important, mediating its localization and association with the C2-domain protein Inn1p at the division site (Jendretzki *et al.*, 2009; Nishihama *et al.*, 2009). Similarly, the SH3 domain of the *S. cerevisiae* F-BAR protein Hof1p also propagates an interaction with Inn1p (Jendretzki *et al.*, 2009; Nishihama *et al.*, 2009; Meitinger *et al.*, 2010). However, whereas loss of Inn1p typically results in lethality or extremely poor growth (Sanchez-Diaz *et al.*, 2008; Jendretzki *et al.*, 2009; Nishihama *et al.*, 2009), *cyk3*Δ or *hof1*Δ cells show relatively minor defects in cytokinesis and growth (Kamei *et al.*, 1998; Lippincott and Li, 1998; Korinek *et al.*, 2000). Moreover, reminiscent of the lethal phenotype of a *cyk3*Δ *hof1*Δ double mutant, a double mutant possessing truncated forms of both Cyk3p and Hof1p (lacking their SH3 domains) does not grow (Jendretzki *et al.*, 2009). In contrast, in fission yeast,

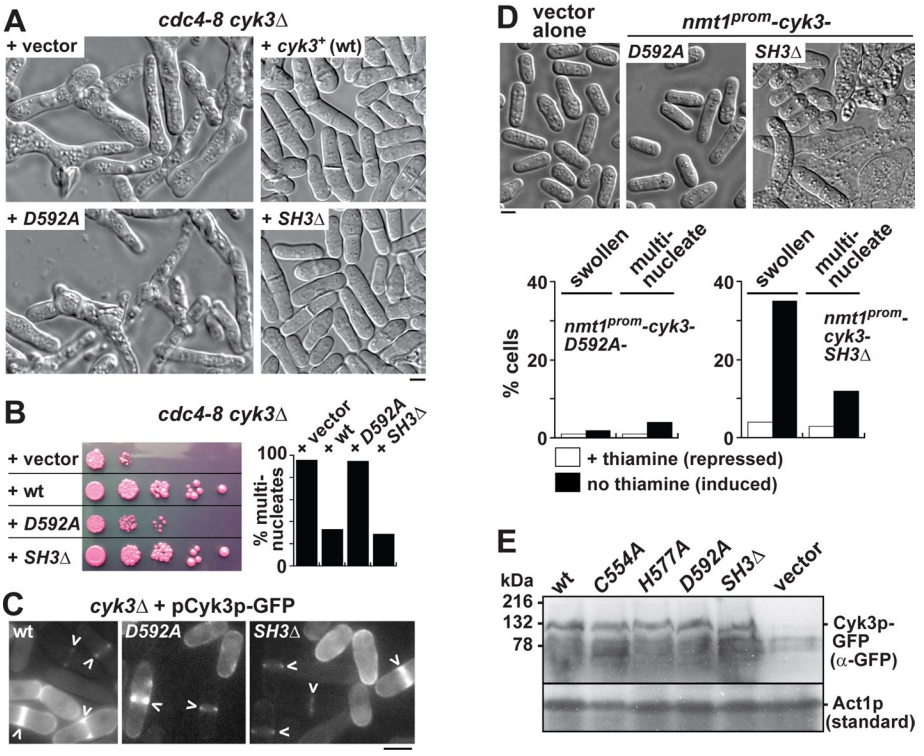

FIGURE 8: Cyk3p function depends on its transglutaminase domain but not its SH3 domain. (A and B) Rescue of the *cdc4-8 cyk3Δ* synthetic phenotype by plasmids expressing wild-type Cyk3p-GFP or Cyk3p-SH3Δ-GFP but not by vector alone or a plasmid expressing Cyk3p-Asp-592-Ala-GFP. *cdc4-8 cyk3Δ* cells (MLP 178) were transformed with plasmid *pGFP* (vector control), *cyk3-GFP*, *cyk3-SH3Δ-GFP*, or *cyk3-Asp-592-Ala-GFP* (see Table 3 and *Materials and Methods*). (A) Representative fields of cells were imaged by DIC microscopy after growth in EMM-uracil liquid medium at 32°C (used because the restrictive temperature of the *cdc4-8 cyk3Δ* double mutant is higher in minimal than in rich medium). (B) Left, 5-μl aliquots of cell suspensions (of identical optical density) were spotted along with four 10-fold serial dilutions of each onto EMM- uracil plates containing 5 μg/ml phloxin B and grown at 30°C. Right, the cultures described in (A) were scored for cytokinetic defects (as percentages of multinucleate cells; n = 500). (C) Normal localization of wild-type and mutant forms of Cyk3p-GFP to contractile rings (arrowheads). *cyk3Δ* transformants were grown in EMM-uracil liquid medium at 25°C. The variable strength of the Cyk3p-GFP signal presumably reflects the variable copy number of fission yeast plasmids. (D) Effects of overexpressing mutant forms of Cyk3p. Wild-type strain MLP 11 was transformed with plasmid *nmt1prom-cyk3-SH3Δ* or *nmt1prom-cyk3-Asp-592-Ala* (Table 3), and were then grown and scored as described in Figure 7. Top, representative DIC images; bottom, quantification of morphological defects (n = 500). (E) Wild-type and mutant forms of Cyk3p-GFP are expressed at similar levels. *cyk3Δ* strain MLP 3 was transformed with plasmids expressing the indicated proteins and grown as in (C). Extracts were prepared, normalized for total protein, and evaluated by immunoblotting using anti-GFP or anti-actin (as a loading control) antibodies. The indicated band has the appropriate apparent molecular weight (~125 kDa) for a full-length Cyk3p-GFP fusion; as expected, the Cyk3p-SH3Δ-GFP fusion runs slightly faster. Scale bars: 4 μm.

the Cyk3p SH3 domain is not critical for function and does not share a redundant role with the SH3 domains of the F-BAR proteins Cdc15p and Imp2p. Irrespective of the status of Cyk3p, removal of the SH3 domains from both F-BAR proteins is enough to prevent recruitment of the C2-domain protein Fic1p to the division site (Roberts-Galbraith *et al.*, 2009).

Although its SH3 domain is dispensable, the fission yeast Cyk3p TGase domain is required for function (an issue that does not appear to have been investigated for the *S. cerevisiae* protein). Each of the conserved active-site residues cysteine, histidine, and aspartic acid, which make up the catalytic triad at the core of TGases, is essential for enzymatic activity (Hettasch and Greenberg, 1994; Micanovic *et al.*, 1994; Pedersen *et al.*, 1994; Yee *et al.*, 1994), and mutagenesis of the corresponding aspartic acid (Asp-592) or histidine (His-577) residues of fission yeast Cyk3p led to complete or partial loss of function, respectively. Although these results demonstrate the importance of the TGase domain, it cannot function enzymatically because it lacks the cysteine residue to complete the catalytic triad (Figure 1A). The nearest cysteine residue (Cys-554) is 18 amino acids downstream from where the catalytic cysteine would be expected (Figure 1A). Nonetheless, this cysteine is conserved among Cyk3p homologues (Figure 1A) and could theoretically form a catalytic triad with His-577 and Asp-592. However, analysis of a Cys-554-Ala point mutant indicated that this was not the case. The Cys-554-Ala protein was expressed normally and behaved just like wild-type Cyk3p in vivo (Figures 8E and S4). In addition, the fact Cyk3p-His-577-Ala (but not -Asp-592-Ala) retains partial function (as opposed to complete loss or full function) also argues against an enzymatic role for the TGase domain in Cyk3p function.

The inactive nature of the Cyk3p TGase domain may reflect a structural/cytoskeletal role for this domain in cell wall remodeling, in which the charged His-577 and Asp-592 residues could help mediate electrostatic interactions between the TGase domain and Cyk3p binding partners. Similarly, a structural role has been proposed for band 4.2, the inactive TGase implicated in human disease that functions at the membrane of red blood cells (Satchwell *et al.*, 2009). Alternatively, the inactive Cyk3p TGase domain may be a mimic that functions as a dominant-negative regulator of other TGases. In this case, the localization of Cyk3p to sites of cell wall remodeling may promote cell wall dynamics and plasticity by sequestering substrates and thus limiting their cross-linking and stabilization by active endogenous TGases. This hypothesis is supported by the observations that TGase-mediated cross-linking contributes to cell wall organization in *S. cerevisiae* (Iranzo *et al.*, 2002), *C. albicans* (Ruiz-Herrera *et al.*, 1995), and the green alga *Chlamydomonas reinhardtii* (Waffenschmidt *et al.*, 1999). Inhibition of cell wall cross-linking by Cyk3p might explain why its overexpression leads to the loss of polarity and ballooning of cells that could accompany loss of rigidity/excessive plasticity within the cell wall.

In conclusion, our work on fission yeast Cyk3p highlights the importance of the inactive subclass of the TGases that are found throughout eukaryotes. Animal TGases are thought to have evolved from bacterial thiol proteases, because they utilize the same catalytic triad and share the same core structural fold (Pedersen *et al.*, 1994; Yee *et al.*, 1994). Thus, in addition to adaptations favoring substrate cross-linking (via a reversion of the proteolytic reaction), adaptations associated with loss of enzymatic activity also appear to have been selected during the course of evolution.

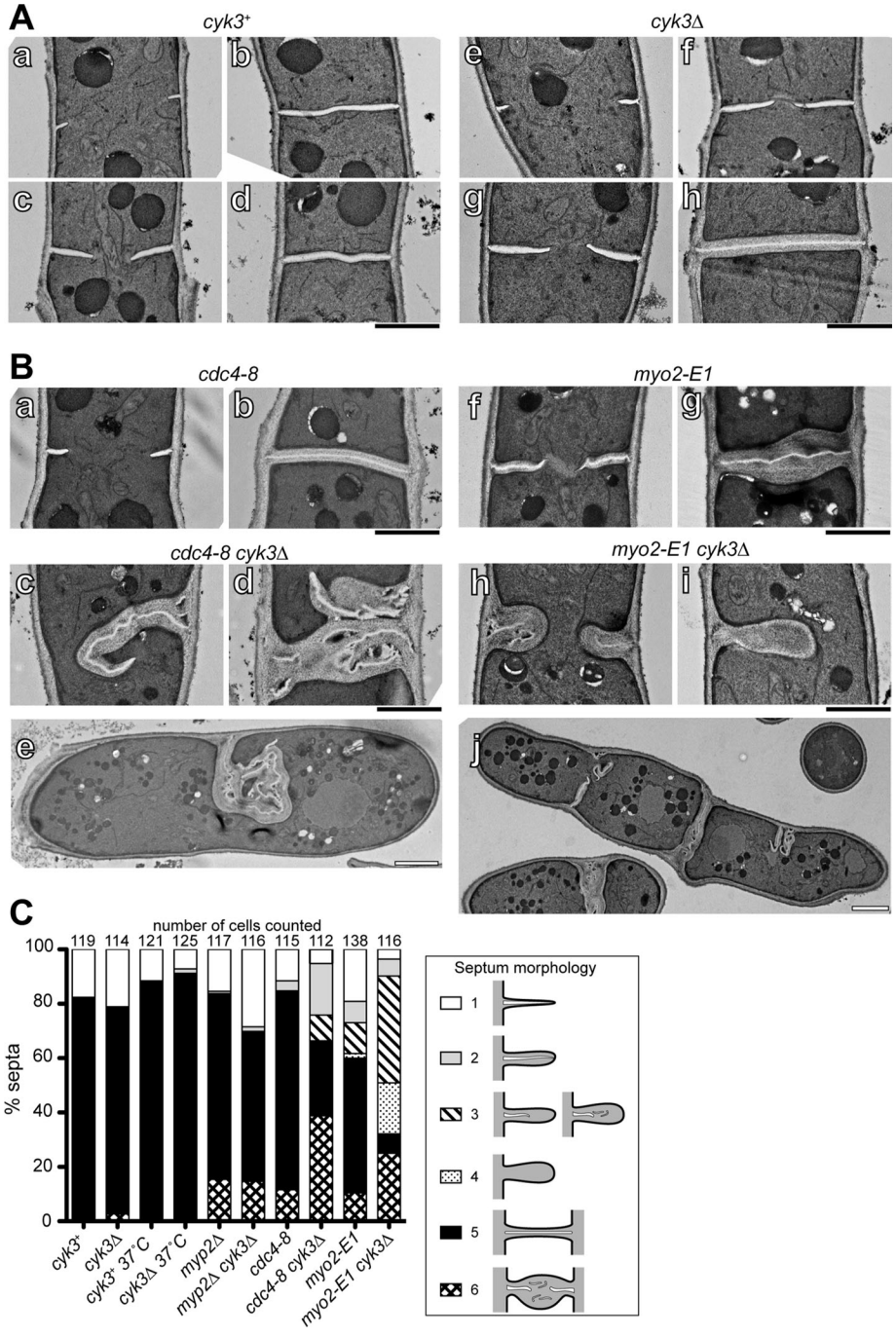

FIGURE 9: EM analysis of septation with and without Cyk3p. (A) Deletion of *cyk3* alone has a mild effect on septum morphology. Representative electron micrographs of wild-type (a–d) and *cyk3Δ* (e–h) cells grown at 27.5°C in YE5S medium are shown. Cells in the initial (a and e) and late (b, c, f, and g) stages of septation are shown, as are cells with complete septa (d and h). Scale bars: 0.5 µm. (B) Deletion of *cyk3* exacerbates the septum morphology defects in *cdc4-8* (a–e) and *myo2-E1* (f–j) mutants. Cells were cultured as in (A); representative images are shown. Black scale bars: 0.5 µm; white scale bars (e and j): 2 µm. (C) Quantitative analysis of septum morphology in wild-type and mutant strains. Cells were grown in YE5S medium at 27.5°C, except for two cultures that were incubated at 37°C for 4 h following overnight growth at 25°C. The septa observed by EM were classified as follows: 1, an incomplete sharp septum with an electron-translucent (white) band reaching its leading edge; 2, an incomplete bulged septum with a white band reaching its leading edge; 3, an incomplete bulged septum with a white band(s) not reaching its leading edge; 4, an incomplete bulged septum with no white band; 5, a complete septum across the division plane; 6, a complete but deformed septum with interrupted white bands.

MATERIALS AND METHODS

Fission yeast strains, plasmids, and genetic methods

Strains were grown in EMM (Edinburgh minimal media) or YE5S (yeast extract plus supplements) medium, and standard genetic and cell biology protocols were used (Moreno *et al.*, 1991). Table 2 lists the strains used in this study. Gene deletion mutants and strains expressing fusion proteins tagged with GFP, 3GFP, or Cherry were constructed using genomic integrations with the relevant kan^R or nat^R cassettes (Bahler *et al.*, 1998). Cyk3p-GFP and Cyk3p-3GFP fusions were functional based on their ability to fully support Cyk3p function in a *cdc4-8* background. Plasmids used in this study are listed in Table 3. The *cyk3* open reading frame (ORF) was amplified from a genomic library using the primers: 5′ *Xho*I-*cyk3 CTCGAG*ATGTCCATTCCTAAACAACTACCATGC; 3′ *Not*I-*cyk3 GCGGCCGC*CAACCGCCTGCCAGGTTGCATAGC. The ORF was ligated into *Xho*I/*Not*I-linearized pDS572a (overexpression vector with the *nmt1* high-strength promoter) and pDS572-81 (*nmt1-81* weak-strength promoter vector for plasmid-based complementation). A Cyk3p N-terminal truncation construct lacking amino acids 3–65 (spanning the entire SH3 domain and seven upstream residues) was made using the 5′ primer: *Xho*I-*cyk3-SH3Δ*: *CTCGAG*ATGAGTGATATTCCCACGGTACGACCTGGC. A Cyk3p Asp-592-Ala point mutant was constructed using overlap extension (Ho *et al.*, 1989) to amplify a mutated 3′ 800–base pair fragment of the *cyk3* ORF. Overlapping subfragments were generated using the following primers: 1) 5′ *Ssp*I-*cyk3*: CTGTAGGTACT*AATATT*CATAACATG and 3′ Asp-592-Ala: GGCAAAACTAGCAGCAATTAGACG; and 2) 5′ Asp-592-Ala: CGTCTAATTGCTGCTAGTTTTGCC and 3′ *Hpa*I-*cyk3*: GTTTCCCAGAAAGCCTGT*GTTAAC*GTG. The mutant fragment was amplified from the overlapping fragments (using the 5′ *Ssp*I and 3′ *Hpa*I primers) and subcloned into a Topo-*cyk3* clone via the unique *Ssp*I and *Hpa*I sites (which reside in the 3′ region of the *cyk3* ORF). The mutated *cyk3* ORFs were inserted into the pDS572a and pDS572-81 vectors. The same strategy was used to generate Cyk3p-Cys-554-Ala and -His-577-Ala mutants with the following primers (and their 3′ complements): 5′ Cys-554-Ala: GCACTAGATTTATGGGCTGAGGTTATCG and 5′ His-577-Ala: CCAGAGATATTAATATAAATGCTGCTTGGAATG. The fidelity of *cyk3* sequences was confirmed by DNA sequencing.

Strain	Genotype	Source
TP 6	*h⁺ leu1-32 his7-366 ade6-M216 cdc4-8*	M. Balasubramanian[a]
TP 19	*h⁻ leu1-32 ura4-D18 his7-366 ade6-M216 cdc12-112*	M. Balasubramanian[a]
TP 30	*h⁺ leu1-32 ura4-D18 his7-366 ade6-M210 cdc15-127*	M. Balasubramanian[a]
TP 73	*h⁻ leu1-32 ura4-D18 his7-366 ade6-M216 myo2-E1*	M. Balasubramanian[a]
MLP 3	*h⁺ leu1-32 ura4-D18 his7-366 ade6-M210 cyk3Δ::kan^R*	This study
MLP 11	*h⁺ leu1-32 ura4-D18 his7-366 ade6-M210*	This study
MLP 15	*h⁺ leu1-32 ura4-D18 his7-366 ade6-M210 cyk3-^{m}GFP::kan^R*	This study
MLP 17	*h⁻ leu1-32 ura4-D18 his7-366 ade6-M210 myo2-E1 cyk3Δ::kan^R*	This study
MLP 18	*h⁻ leu1-32 ura4-D18 his7-366 ade6-M216 cyk3Δ::kan^R*	This study
MLP 34	*h⁺ leu1-32 ura4-D18 his7-366 ade6-M210 myp2Δ::his7⁺*	T. Pollard
MLP 35	*h⁻ leu1-32 ura4-D18 his7-366 ade6-M210 myp2Δ::his7⁺ cyk3Δ::kan^R*	This study
MLP 178	*h⁻ leu1-32 ura4-D18 his7-366 ade6-M210 cdc4-8 cyk3Δ::kan^R*	This study
MLP 198	*h⁺ leu1-32 ura4-D18 his7-366 ade6-M210 rlc1-^{m}GFP:kan^R*	This study
MLP 319	*h⁻ leu1-32 ura4-D18 his7-366 ade6-M216 myo2-E1 rlc1-^{m}GFP:kan^R*	This study
MLP 323	*h⁻ leu1-32 ura4-D18 his7-366 ade6 cdc12-112 cyk3Δ::kan^R*	This study
MLP 326	*h⁻ leu1-32 ura4-D18 his7-366 ade6 cdc15-127 cyk3Δ::kan^R*	This study
MLY 572	*h⁻ leu1-32 ura4-D18 ade6 his3-D1 rlc1-^{m}GFP:kan^R sad1-^{m}GFP:kan^R*	This study
MLY 655	*h⁻ leu1-32 ura4-D18 his7-366 ade6 cyk3Δ::kan^R rlc1-^{m}GFP:kan^R*	This study
MLY 657	*h⁻ leu1-32 ura4-D18 ade6 his3-D1 cyk3Δ::kan^R rlc1-^{m}GFP:kan^R sad1-^{m}GFP:kan^R*	This study
MLY 757	*h⁻ leu1-32 ura4-D18 his3-D1 ade6 cyk3-3xGFP::kan^R rlc1-Cherry::nat^R*	This study
LP 33	*h⁻ leu1-32 ura4-D18 his3-D1 ade6 cyk3-3xGFP::kan^R fim1-Cherry::nat^R*	This study
LP 37	*h⁺ leu1-32 ura4-D18 his3-D1 ade6 cyk3-3xGFP::kan^R*	This study
LP 69	*h⁻ leu1-32 ura4-D18 his3-D1 ade6 sid2-250 cyk3-3xGFP::kan^R rlc1-Cherry::nat^R*	This study
LP 109	*h⁺ leu1-32 ura4-D18 his7-366 ade6-M216 myo2-E1 cyk3Δ::kan^R rlc1-^{m}GFP:kan^R*	This study
LP 112	*h⁻ leu1-32 ura4-D18 his3-D1 ade6 chs2Δ::ura4⁺ cyk3Δ::kan^R*	This study
LP 116	*h⁺ leu1-32 ura4-D18 his3-D1 ade6 cdc25-22 cyk3-3xGFP::kan^R rlc1-Cherry::nat^R*	This study
HVP 280	*h⁻ leu1-32 ura4-D18 his3-D1 ade6 chs2Δ::ura4⁺*	Henar Valdivieso[b]

[a]Temasek Life Sciences Laboratory, Singapore.
[b] University of Salamanca, Spain.

TABLE 2: Fission yeast strains.

Microscopy

Differential interference contrast (DIC) and epifluorescence cell images were captured using a Nikon (Melville, NY) TE2000-E2 inverted microscope with motorized fluorescence filter turret and a Plan Apo 60×/1.45 numerical aperture (NA) objective. For fluorescence, an EXFO X-CITE 120 illuminator was utilized. NIS Elements software was used to control the microscope, two Uniblitz shutters, a Photometrics CoolSNAP HQ2 14-bit camera, and auto-focusing. Time-lapse movies of cells monitored Cyk3p and/or Rlc1p contractile ring dynamics (every 2–3 min for 2–3 h) and Cyk3p and/or Fim1p cortical patch lifetimes (by capturing images every 5–10 s for 5–10 min) using appropriate filters. For ring movies, autofocusing was performed on the DIC channel before each image capture. Cell suspensions (3 μl) were mounted on flat 30-μl media pads (solidified by 1% agarose) prepared on the slide surface. VALAP (1:1:1 vasoline:lanolin:paraffin) was used to seal slides and coverslips. For simultaneous tracking of SPBs (Sad1p-GFP) and rings (Rlc1p-GFP), a Z-stack of six images (taken every 0.75 μm spanning the depth of the cell) was collected every 2–3 min for 90–120 min. Images were captured using Nikon (Melville, NY) ND software, and analysis of ring and patch dynamics was performed using Image J, Microsoft Excel, and KaleidaGraph software. Ring dynamics were quantified by assessing individual phases: *assembly* was time taken for Rlc1p-GFP to compact into a mature ring following its appearance as a broad band of nodes; *dwell* was time from completion of ring compaction until initiation of constriction; *constriction* was change in ring circumference over time. Dwell times and constriction initiation were discerned by plotting ring diameter over time for each ring, and constriction rates were derived from the slopes of these plots.

FRAP experiments used confocal laser-scanning microscopy with a Zeiss LSM 510 META system equipped with an argon laser, META detector, and a Plan-Apo 100×/1.4 NA objective. Cells were mounted on 1% agarose pads (as described above) prior to microscopy at room temperature. A region of interest (ROI) was selected on Cyk3p-GFP rings for directed bleaching. Photobleaching iterations were performed briefly at high laser power, resulting in

Plasmid	Comment	Source
pFA6a-kanMX6	Template for gene replacement with a *kan*^{R} cassette	Bahler *et al.*, 1998
pFA6a-kanMX6/ nat^R-^{m}GFP/ -3xGFP/-Cherry	Templates for integration of C-terminal tags into the genome	J.-Q. Wu [a] W.-L. Lee[b] V. Sirotkin[c]
nmt1^{prom}	pDS572a (*nmt1* promoter, C-terminal GFP, *ura4*$^+$)	S. Forsburg[d]
nmt1^{prom}-cyk3	pDS572a harboring wild-type *cyk3*	This study
nmt1^{prom}-cyk3-Asp-592A	pDS572a harboring *cyk3-Asp-592-Ala*	This study
nmt1^{prom}-cyk3-His-577A	pDS572a harboring *cyk3-His-577-Ala*	This study
nmt1^{prom}-cyk3-Cys-554A	pDS572a harboring *cyk3-Cys-554-Ala*	This study
nmt1^{prom}-cyk3-SH3Δ	pDS572a harboring *cyk3-SH3Δ*	This study
pGFP	pDS572-81 (*nmt1-81x* promoter, C-terminal GFP, *ura4*$^+$)	S. Forsburg[d]
cyk3-GFP	pDS572-81 harboring wild-type *cyk3*	This study
cyk3-Asp-592A-GFP	pDS572-81 harboring *cyk3-Asp-592-Ala*	This study
cyk3-His-577A-GFP	pDS572-81 harboring *cyk3-His-577-Ala*	This study
cyk3-Cys-554A-GFP	pDS572-81 harboring *cyk3-Cys-554-Ala*	This study
cyk3-SH3Δ-GFP	pDS572-81 harboring *cyk3-SH3Δ*	This study

[a]Ohio State University, Columbus, OH.
[b]University of Massachusetts, Amherst, MA.
[c]SUNY Upstate Medical University, Syracuse, NY.
[d]University of Southern California, Los Angeles, CA.

TABLE 3: Plasmids.

~90–100% signal loss. Signal recovery was monitored by time-lapse analysis at low laser power, with images collected every 5 s postbleach until the recovery signal plateaued (~2 min). The criterion for determining whether Cyk3p rings were constricting or not lay in their diameters: if rings were clearly narrower than the cell diameter, we scored them as constricting; if they were the same diameter as the cell width, we viewed them as nonconstricting. The LSM 510 software (version 4.2) was used to collect images and perform data analysis (see Figure 4B legend). Recovery curves of Cyk3p-GFP signal versus time were plotted and fit using KaleidaGraph software. Data sets for each trace were corrected for any additional bleaching encountered during time-lapse imaging by a control ROI (derived from an unbleached ring in the same field of cells). To facilitate curve fitting, zero signal intensity was set for each trace by subtracting any residual Cyk3p-GFP signal (detected at the first time point postbleach, 0 s) from all trace values. The $t_{½}$ values (± SD) represent the mean generated from the fits of each individual FRAP experiment.

EM was performed as previously described (Nishihama *et al.*, 2009), with minor modifications. Cells were cultured overnight in YE5S medium at 25°C to mid-log phase, diluted to an OD_{600} of 0.1, and then regrown at 27.5°C to an OD_{600} of 0.5 (or at 37°C for 4 h). The cells were harvested, fixed with glutaraldehyde and potassium permanganate, stained with uranyl acetate, and embedded in LR White resin (Fluka, St. Louis, MO). Thin-section samples were post-stained with uranyl acetate and lead citrate and were observed using a JEM1230/JEOL microscope (Tokyo, Japan) equipped with an ORIUS SC1000A cooled-CCD camera (Gatan, Pleasanton, CA).

Western Blotting

cyk3Δ cells harboring *pGFP* (vector alone), *cyk3-GFP*, *cyk3-Asp-592-Ala-GFP*, *cyk3-His-577-Ala-GFP*, *cyk3-Cys-554-Ala-GFP*, or *cyk3-SH3Δ-GFP* plasmids were grown to an OD_{595} of 1 in 200 ml of EMM Ura– medium. Cells were then harvested and washed once in water and once in ice-cold lysis buffer (750 mM KCl, 25 mM Tris-HCl, pH 7.4, 4 mM $MgCl_2$, 20 mM $Na_4P_2O_7$, 2 mM ethylene glycol tetraacetic acid, and 0.1% Triton X-100). Pellets were resuspended in an equal volume of ice-cold lysis buffer with additives consisting of 1 mM dithiothreitol, 4 mM ATP, 2 mM phenylmethylsulfonyl fluoride, and complete EDTA-free protease inhibitors (Roche, Indianapolis, IN). From this point forward, all work was performed at 4°C and samples were stored on ice. Cells were lysed by glass bead beating with a Fastprep (MP Biochemicals, Solon, OH). Lysates were normalized for total protein using a Bradford mix (Bio-Rad, Hercules, CA), mixed 1:1 with 2X SDS–PAGE loading buffer, and boiled for 10 min. Samples were run on a 10% SDS–PAGE gel, transferred to nitrocellulose, and immunoblotted (Sambrook *et al.*, 1989) using anti-GFP (Clontech, Mountain View, CA) and anti-actin (Chemicon, Temecula, CA) antibodies diluted 1:1000 in PBS containing 0.1% Tween-20. Horse radish peroxidase-conjugated secondary antibodies were used (diluted 1:3000).

ACKNOWLEDGMENTS

We thank Mohan Balasubramanian (Temasek Life Sciences Laboratory, Singapore) for the *cdc4-8*, *cdc12-112*, *cdc15-127*, *myo2-E1*, and *sid2-250* strains; Jian-Qiu Wu (Ohio State University, Columbus, OH) for the *cdc25-22* strain; Henar Valdivieso (University of Salamanca, Spain) for the *chs2Δ* strain; and Tom Pollard (Yale University, New Haven, CT) for the *myp2Δ* strain. We thank Wei-Lee Li (University of Massachusetts, Amherst, MA), Volodia Sirotkin (SUNY Upstate Medical University, Syracuse, NY), Jian-Qiu Wu, and Susan Forsburg (University of Southern California, Los Angeles, CA) for pFA6a derivatives and fission yeast plasmids. We are very grateful to Tom Pollard, within whose laboratory this work was initiated. Work in the Lord laboratory is funded by an American Heart Association Scientist Development Grant (0835236N) and a National Institutes of Health grant (GM097193); yeast work in the Pringle laboratory has been funded by the National Institutes of Health grant GM31006.

REFERENCES

Bahler J, Wu JQ, Longtine MS, Shah NG, McKenzie A, III, Steever AB, Wach A, Philippsen P, Pringle JR (1998). Heterologous modules for efficient and versatile PCR-based gene targeting in *Schizosaccharomyces pombe*. Yeast 14, 943–951.

Bezanilla M, Forsburg SL, Pollard TD (1997). Identification of a second myosin-II in *Schizosaccharomyces pombe*: Myp2p is conditionally required for cytokinesis. Mol Biol Cell 8, 2693–2705.

Bezanilla M, Wilson JM, Pollard TD (2000). Fission yeast myosin-II isoforms assemble into contractile rings at distinct times during mitosis. Curr Biol 10, 397–400.
Bruce LJ, Ghosh S, King MJ, Layton DM, Mawby WJ, Stewart GW, Oldenborg PA, Delaunay J, Tanner MJ (2002). Absence of CD47 in protein 4.2-deficient hereditary spherocytosis in man: an interaction between the Rh complex and the band 3 complex. Blood 100, 1878–1885.
Cohen CM, Dotimas E, Korsgren C (1993). Human erythrocyte membrane protein band 4.2 (pallidin). Semin Hematol 30, 119–137.
Dahl KN, Parthasarathy R, Westhoff CM, Layton DM, Discher DE (2004). Protein 4.2 is critical to CD47-membrane skeleton attachment in human red cells. Blood 103, 1131–1136.
Dekker N, Speijer D, Grun CH, van den Berg M, de Haan A, Hochstenbach F (2004). Role of the α-glucanase Agn1p in fission-yeast cell separation. Mol Biol Cell 15, 3903–3914.
Facchiano F, Facchiano A, Facchiano AM (2006). The role of transglutaminase-2 and its substrates in human diseases. Front Biosci 11, 1758–1773.
Fankhauser C, Reymond A, Cerutti L, Utzig S, Hofmann K, Simanis V (1995). The S. pombe *cdc15* gene is a key element in the reorganization of F-actin at mitosis. Cell 82, 435–444.
Fesus L, Szondy Z (2005). Transglutaminase 2 in the balance of cell death and survival. FEBS Lett 579, 3297–3302.
Herman PK (2002). Stationary phase in yeast. Curr Opin Microbiol 5, 602–607.
Hettasch JM, Greenberg CS (1994). Analysis of the catalytic activity of human factor XIIIa by site-directed mutagenesis. J Biol Chem 269, 28309–28313.
Ho SN, Hunt HD, Horton RM, Pullen JK, Pease LR (1989). Site-directed mutagenesis by overlap extension using the polymerase chain reaction. Gene 77, 51–59.
Iranzo M, Aguado C, Pallotti C, Canizares JV, Mormeneo S (2002). Transglutaminase activity is involved in *Saccharomyces cerevisiae* wall construction. Microbiology 148, 1329–1334.
Jendretzki A, Ciklic I, Rodicio R, Schmitz HP, Heinisch JJ (2009). Cyk3 acts in actomyosin ring independent cytokinesis by recruiting Inn1 to the yeast bud neck. Mol Genet Genomics 282, 437–451.
Kamei T, Tanaka K, Hihara T, Umikawa M, Imamura H, Kikyo M, Ozaki K, Takai Y (1998). Interaction of Bnr1p with a novel Src homology 3 domain-containing Hof1p. Implication in cytokinesis in *Saccharomyces cerevisiae*. J Biol Chem 273, 28341–28345.
Knox P, Crooks S, Rimmer CS (1986). Role of fibronectin in the migration of fibroblasts into plasma clots. J Cell Biol 102, 2318–2323.
Korinek WS, Bi E, Epp JA, Wang L, Ho J, Chant J (2000). Cyk3, a novel SH3-domain protein, affects cytokinesis in yeast. Curr Biol 10, 947–950.
Korsgren C, Lawler J, Lambert S, Speicher D, Cohen CM (1990). Complete amino acid sequence and homologies of human erythrocyte membrane protein band 4.2. Proc Natl Acad Sci USA 87, 613–617.
Lippincott J, Li R (1998). Dual function of Cyk2, a cdc15/PSTPIP family protein, in regulating actomyosin ring dynamics and septin distribution. J Cell Biol 143, 1947–1960.
Makarova KS, Aravind L, Koonin EV (1999). A superfamily of archaeal, bacterial, and eukaryotic proteins homologous to animal transglutaminases. Protein Sci 8, 1714–1719.
Mangala LS, Mehta K (2005). Tissue transglutaminase (TG2) in cancer biology. Prog Exp Tumor Res 38, 125–138.
Martin-Cuadrado AB, Duenas E, Sipiczki M, Vazquez de Aldana CR, del Rey F (2003). The endo-β-1,3-glucanase eng1p is required for dissolution of the primary septum during cell separation in *Schizosaccharomyces pombe*. J Cell Sci 116, 1689–1698.
Martin-Garcia R, Duran A, Valdivieso MH (2003). In *Schizosaccharomyces pombe* chs2p has no chitin synthase activity but is related to septum formation. FEBS Lett 549, 176–180.
Martin-Garcia R, Valdivieso MH (2006). The fission yeast Chs2 protein interacts with the type-II myosin Myo3p and is required for the integrity of the actomyosin ring. J Cell Sci 119, 2768–2779.
McCollum D, Gould KL (2001). Timing is everything: regulation of mitotic exit and cytokinesis by the MEN and SIN. Trends Cell Biol 11, 89–95.
Mehta K, Kumar A, Kim HI (2010). Transglutaminase 2: a multi-tasking protein in the complex circuitry of inflammation and cancer. Biochem Pharmacol 80, 1921–1929.
Meitinger F, Petrova B, Lombardi IM, Bertazzi DT, Hub B, Zentgraf H, Pereira G (2010). Targeted localization of Inn1, Cyk3 and Chs2 by the mitotic-exit network regulates cytokinesis in budding yeast. J Cell Sci 123, 1851–1861.
Micanovic R, Procyk R, Lin W, Matsueda GR (1994). Role of histidine 373 in the catalytic activity of coagulation factor XIII. J Biol Chem 269, 9190–9194.
Mishra M, Karagiannis J, Trautmann S, Wang H, McCollum D, Balasubramanian MK (2004). The Clp1p/Flp1p phosphatase ensures completion of cytokinesis in response to minor perturbation of the cell division machinery in *Schizosaccharomyces pombe*. J Cell Sci 117, 3897–3910.
Moreno S, Klar A, Nurse P (1991). Molecular genetic analysis of fission yeast Schizosaccharomyces pombe. Methods Enzymol 194, 795–823.
Mosher DF, Schad PE (1979). Cross-linking of fibronectin to collagen by blood coagulation Factor XIIIa. J Clin Invest 64, 781–787.
Motegi F, Nakano K, Kitayama C, Yamamoto M, Mabuchi I (1997). Identification of Myo3, a second type-II myosin heavy chain in the fission yeast *Schizosaccharomyces pombe*. FEBS Lett 420, 161–166.
Mulvihill DP, Hyams JS (2003). Role of the two type II myosins, Myo2 and Myp2, in cytokinetic actomyosin ring formation and function in fission yeast. Cell Motil Cytoskeleton 54, 208–216.
Nishihama R *et al*. (2009). Role of Inn1 and its interactions with Hof1 and Cyk3 in promoting cleavage furrow and septum formation in *S. cerevisiae*. J Cell Biol 185, 995–1012.
Pedersen LC, Yee VC, Bishop PD, Le Trong I, Teller DC, Stenkamp RE (1994). Transglutaminase factor XIII uses proteinase-like catalytic triad to crosslink macromolecules. Protein Sci 3, 1131–1135.
Pisano JJ, Finlayson JS, Peyton MP (1968). Cross-link in fibrin polymerized by factor 13: ε-(γ-glutamyl)lysine. Science 160, 892–893.
Rajagopalan S, Wachtler V, Balasubramanian M (2003). Cytokinesis in fission yeast: a story of rings, rafts and walls. Trends Genet 19, 403–408.
Reijnst P, Jorde S, Wendland J (2010). *Candida albicans* SH3-domain proteins involved in hyphal growth, cytokinesis, and vacuolar morphology. Curr Genet 56, 309–319.
Rice RH, Green H (1978). Relation of protein synthesis and transglutaminase activity to formation of the cross-linked envelope during terminal differentiation of the cultured human epidermal keratinocyte. J Cell Biol 76, 705–711.
Rincon SA, Santos B, Perez P (2006). Fission yeast Rho5p GTPase is a functional paralogue of Rho1p that plays a role in survival of spores and stationary-phase cells. Eukaryot Cell 5, 435–446.
Roberts-Galbraith RH, Chen JS, Wang J, Gould KL (2009). The SH3 domains of two PCH family members cooperate in assembly of the *Schizosaccharomyces pombe* contractile ring. J Cell Biol 184, 113–127.
Roberts-Galbraith RH, Ohi MD, Ballif BA, Chen JS, McLeod I, McDonald WH, Gygi SP, Yates JR, III, Gould KL (2010). Dephosphorylation of F-BAR protein Cdc15 modulates its conformation and stimulates its scaffolding activity at the cell division site. Mol Cell 39, 86–99.
Ruiz-Herrera J, Iranzo M, Elorza MV, Sentandreu R, Mormeneo S (1995). Involvement of transglutaminase in the formation of covalent cross-links in the cell wall of *Candida albicans*. Arch Microbiol 164, 186–193.
Sakata Y, Aoki N (1980). Cross-linking of alpha 2-plasmin inhibitor to fibrin by fibrin-stabilizing factor. J Clin Invest 65, 290–297.
Sambrook J, Fritsch EF, Maniatis T (1989). Molecular Cloning: A Laboratory Manual, Cold Spring Harbor, NY: Cold Spring Harbor Laboratory Press.
Sanchez-Diaz A, Marchesi V, Murray S, Jones R, Pereira G, Edmondson R, Allen T, Labib K (2008). Inn1 couples contraction of the actomyosin ring to membrane ingression during cytokinesis in budding yeast. Nat Cell Biol 10, 395–406.
Satchwell TJ, Shoemark DK, Sessions RB, Toye AM (2009). Protein 4.2: a complex linker. Blood Cells Mol Dis 42, 201–210.
Schwartz ML, Pizzo SV, Hill RL, McKee PA (1973). Human factor XIII from plasma and platelets. Molecular weights, subunit structures, proteolytic activation, and cross-linking of fibrinogen and fibrin. J Biol Chem 248, 1395–1407.
Sirotkin V, Berro J, Macmillan K, Zhao L, Pollard TD (2010). Quantitative analysis of the mechanism of endocytic actin patch assembly and disassembly in fission yeast. Mol Biol Cell 21, 2894–2904.
Sladewski TE, Previs MJ, Lord M (2009). Regulation of fission yeast myosin-II function and contractile ring dynamics by regulatory light-chain and heavy-chain phosphorylation. Mol Biol Cell 20, 3941–3952.
Stark BC, Sladewski TE, Pollard LW, Lord M (2010). Tropomyosin and myosin-II cellular levels promote actomyosin ring assembly in fission yeast. Mol Biol Cell 21, 989–1000.
Thacher SM, Rice RH (1985). Keratinocyte-specific transglutaminase of cultured human epidermal cells: relation to cross-linked envelope formation and terminal differentiation. Cell 40, 685–695.
Waffenschmidt S, Kusch T, Woessner JP (1999). A transglutaminase immunologically related to tissue transglutaminase catalyzes cross-linking of cell wall proteins in *Chlamydomonas reinhardtii*. Plant Physiol 121, 1003–1015.
Yawata Y (1994). Band 4.2 abnormalities in human red cells. Am J Med Sci 307, 190–203.
Yee VC, Pedersen LC, Le Trong I, Bishop PD, Stenkamp RE, Teller DC (1994). Three-dimensional structure of a transglutaminase: human blood coagulation factor XIII. Proc Natl Acad Sci USA 91, 7296–7300.
Zemskov EA, Janiak A, Hang J, Waghray A, Belkin AM (2006). The role of tissue transglutaminase in cell-matrix interactions. Front Biosci 11, 1057–1076.